Preprint. Citation: Martínez-Casasnovas, J.A., Llorens, J., Sandonís, L., Escolà, A., Arnó, J., 2021. NDVI from satellite images to estimate LiDAR-derived geometric and structural parameters in super-intensive almond orchards. In: Stafford, J.V. (ed.), Precision Agriculture'21. Wageningen Academic Publishers, Amsterdam (The Netherlands), pp 567-572. DOI: 10.3920/978-90-8686-916-9

NDVI from satellite images to estimate LiDAR-derived geometric and structural parameters in super-intensive almond orchards

J.A. Martínez-Casasnovas*, J. Llorens, L. Sandonís, A. Escolà, J. Arnó.
Research Group in AgroICT & Precision Agriculture (GRAP), Universitat de Lleida - Agrotecnio Center, E25198, Catalonia, Spain
joseantonio.martinez@udl.cat

Abstract

LiDAR is an effective tool to acquire accurate 3D geometric and structural data in orchards. On the other hand, the temporal resolution of detailed satellite images (PlanetScope, Sentinel-2) offers a great opportunity to monitor the vigour of the orchards. However, there is a gap to bridge in research about the estimation of geometric and structural orchard parameters from vegetation indices and, in particular, between LiDAR-derived parameters and multispectral vegetation indices from satellites. In this work, canopy geometric and structural parameters in a super-intensive almond (*Prunus dulcis*) orchard were estimated from the Normalized Difference Vegetation Index (NDVI) derived from PlanetScope (3 m resolution) and Sentinel-2 (10 m resolution) data. The canopy parameters were measured by means of a Velodyne VLP16 LiDAR sensor. The 3D point cloud was summarized along the orchard rows every 0.5 m. At each point, the maximum height and width, the cross-sectional area and the porosity (ratio between not impacted and emitted laser beams towards the canopy) were calculated. The LiDAR-derived parameters were interpolated to respective grids of 3x3 and 10x10 m, coincident with the center of the pixels of the images. The highest correlations were obtained between the NDVI of PlanetScope images and the cross-sectional area of the almond trees (R=0.72) and with the maximum width of the cross-sections (R=0.71). The correlations with the NDVI of the Sentinel-2 images were significantly lower. The results can be considered optimistic, in particular the use of the PlanetScope images to estimate important canopy geometric parameters for the site-specific management of orchards.

Keywords: LiDAR, geometric parameters, almond orchards, NDVI, Sentinel-2, PlanetScope.

Introduction

Intensive almond orchards (*Prunus dulcis*) are currently in expansion because of the increasing potential profitability of this crop due to its high demand and price (Torres-Sánchez et al., 2018, Lorite et al., 2020). Nevertheless, although mechanization and development of machinery for intensive crop management has increased (Bechar & Vigneault, 2016), most of modern orchards are still managed homogeneously, without considering the spatial variability within the plots.
In order to achieve a more sustainable and accurate management of these crops, in recent years techniques such as LiDAR (light detection and ranging) have started to be applied

(Arnó et al., 2013, Escolà et al., 2017, Colaço et al., 2018). This technology has been gaining importance because it allows very precise geometric and structural parameters, such as height, width, volume, leaf density, porosity, etc. to be known (Escolà et al., 2017). This enables the application of more sustainable fertigation strategies, the evaluation of vegetative growth at different dates or the ability to adapt the pruning intensity in order to improve yield production, among other applications. However, LiDAR data is voluminous and there is no commercial software for their processing in agriculture, nor services that offer that information to be used in management decisions, which is still a gap to bridge. In addition, when the main goal is focused on improving orchard monitoring in order to improve management, it would be necessary to acquire LiDAR data with a certain temporal frequency.

On the other hand, today other remote sensing technologies such UAVs provide an unprecedented capacity to monitor the development and dynamics of tree growth and structure through time (Johansen et al., 2018). Some examples exist that merge LiDAR-derived information with multispectral images from unmanned aerial vehicles (UAV) to characterize the structure of vegetation in orchards (Hobart et al., 2020; Jurado et al., 2020). Nevertheless, UAV images usually present alterations in its quality associated with the speed, height or direction of the flight, and also other problems related to the presence of shadows, depending on the azimuth and inclination of the sun at the time of acquisition (Tu et al., 2020). This has implications in the alteration of radiometric values of the images and of the sensed covers. In addition, as in the case of LiDAR, UAV images also involve the management of a large volume of information, which occupies large amounts of memory, increasing the computational requirement of processing power.

Satellite images offer increasingly high temporal and spatial resolution. Specifically, the Sentinel-2 mission (Copernicus Program, European Union) offers a spatial resolution of 10 m and a revisit time of 5 days due to the two satellites of the mission (Sentinel-2A and Sentinel-2B) (ESA, 2015). Other satellites such as the ones of the PlanetScope constellation (Planet Labs Inc.), offer daily images with very high resolutions (up to 3 m) (Planet, 2016). These images, although they are not as detailed as UAV imagery, allow the earth surface to be distinguished and characterized with a high considerable accuracy and high frequency.

Due to the advantages offered by these two missions (high temporal and spatial resolution) it could be interesting to evaluate their adequacy and accuracy to estimate geometric and structural measurements derived from terrestrial LiDAR. These findings would be very encouraging for regular monitoring and decision making about precise orchard management. However, no works have been found in the scientific literature that relate these measurements with information obtained from satellite images.

Accordingly, the main objective of the present work is to explore the possibilities of extracting geometric and/or structural orchard parameters, which are possible to be extracted from LiDAR-based systems, from satellite images. In this case, images from Sentinel-2 and PlanetScope were used.

Materials and methods

Study area

The study area comprised a 0.75 ha block of an almond orchard (*Prunus dulcis* cv Lauranne Avijor) located in Raimat (Catalonia, NE Spain, X 288260, Y 4616100, ETRS 1989 UTM 31 Zone T, Figure 1). It is a super-intensive orchard, with a plantation pattern of 3.2 x 1.5 m (2800 trees ha^{-1}). The tree rows form a continuous and vertical wall (Figure 1). The orchard was planted during the 2016/17 winter. During winter, the orchard is

pruned manually with the objective of creating a hedge of low vigour branches (fine, short with a certain horizontal tendency). Then, at the end of the spring, the orchard is mechanically pruned to maintain an efficient and active exposed leaf area to develop the maximum productive potential, and to facilitate the work of the harvesting machines. The width of the vegetation hedge is adjusted to a distance of about 35 cm on each side of the axis of the tree rows. With that, lighting and aeration conditions of the hedge are improved. In the present study case, the mechanical pruning was done on June 19, 2019.

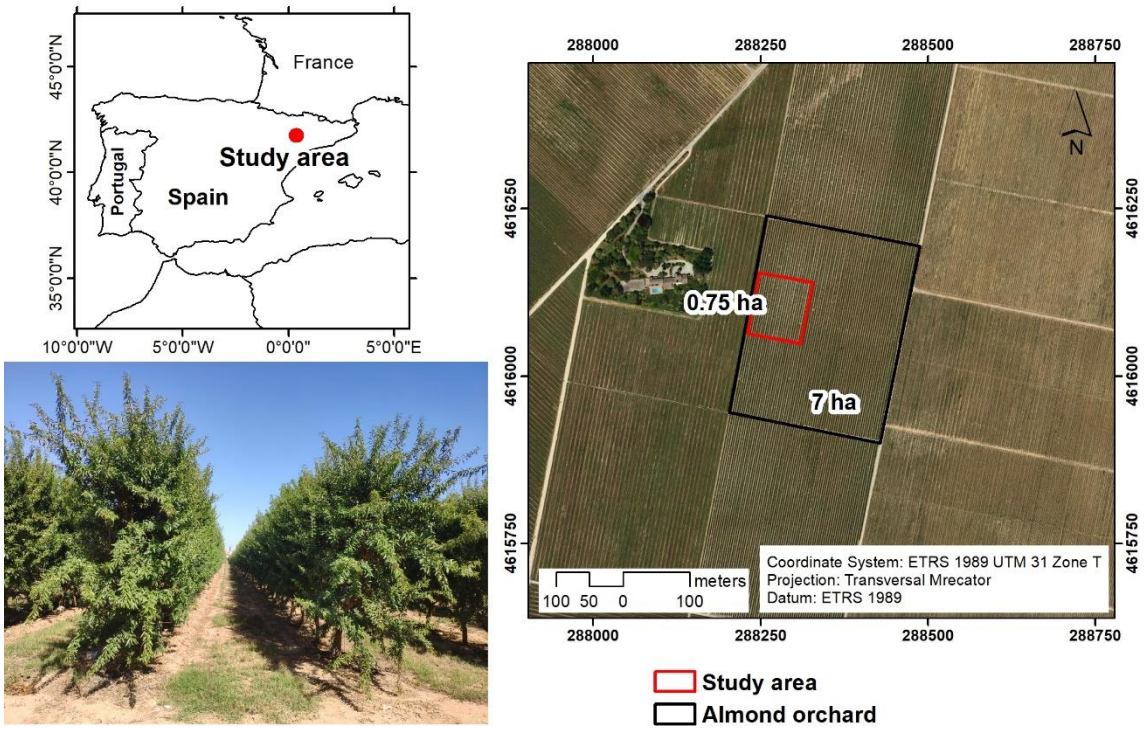

Figure 1. Location of the case study area. Right: almond field and block where LiDAR data was acquired. Bottom left: view of the super-intensive almond orchard.

LiDAR data acquisition and processing

LiDAR data was acquired on June 22nd, 2019 by means of a self-developed mobile terrestrial laser scanner using a VLP-16 LiDAR sensor (Velodyne Lidar Inc., Silicon Valley, USA). This sensor has a range of 100 m and dual return capability. It uses 16 simultaneous laser beams with 30º field of view to acquire ~300,000 points s^{-1} with a 360° scanning window. The LiDAR point data was georeferenced with a Leica GPS 1200 GNSS-RTK system (Leica, Wetzlar, Germany). The LiDAR sensor was mounted in a self-propelled mobile platform moving at a constant speed of 2 km h^{-1}.

Data from 24 tree rows (84 m long each) were acquired during the survey, with a total number of 3D points of 469 million. This point cloud was processed with the aid of RStudio (Version 1.2.5001 using R version 3.6.1 as calculation engine), with an own developed R code described in Llorens et al. (2019). By applying this code, geometric and structural parameters of the canopy were extracted every 0.5 m along the tree rows. For that, this R code first reads the coordinates of the beginning and the end of each ROI-A (region of interest A) that is analysed to extract crop parameters. Once ROI-A is defined, the analysis runs according to smaller ROIs of 0.5 m increments along the Y axis (ROI-B) corresponding to the row axis and increments along the Z axis (ROI-C) (0.10 m in the present case) corresponding to the height of the crop. To reduce the number of points to be analysed, only the central LiDAR beam was used to extract information from

the point cloud. The geometric and structural parameters extracted with this method are summarized in Table 1.

Table 1. Description of the geometric and structural vegetation parameters extracted from the LiDAR point cloud each 0.5 m along the tree row.

Parameter	Description
MaxWidth (m)	Average width of the vegetation row calculated as the average of the maximum widths in each vertical section (0.1 m).
MaxMaxWidth (m)	Maximum width of the vegetation calculated from the most extreme points of the LiDAR points in each analysis zone along the vegetation and without taking into account sections in height.
MaxHeight (m)	Maximum height of the vegetation row in the analysis area.
Schull (m^2)	Vegetation section in each analysis zone calculated using the Convex Hull method (grDevices package in R). This method calculates the surface of a bast polygon that contains the vegetation.
SMaxWidth (m^2)	Cross section calculated according to the maximum width measured at each 0.1 m in height.
Porosity Left, Right and Average (%)	Vegetation wall porosity from both scan sides (Left and Right). It is calculated as the percentage of LiDAR beams that have passed through the vegetation wall in relation to all beams sent from the LiDAR sensor. From the left and right values, the average is calculated.

Satellite data acquisition and processing

Three satellite images were acquired to compute the Normalized Difference Vegetation Index (NDVI, Rouse et al., 1974) and compare it with the parameters extracted from the LiDAR data. These were one Sentinel-2A image (S2A_MSIL2A_20190625T105031_N0212_R051_T31TBG), with 10 m resolution, and two PlanetScope images (20190625_131344_0f02, 20190627_102804_0f17), with 3 m resolution. The images were Bottom-of-Atmosfere (BoA) surface reflectance and projected to the WGS84 UTM 31N, coordinate system, as provided by the Copernicus and Planet Labs services. After calculation of the NDVI, the ones of the PlanetScope images (June 25th and June 27th, 2019) were averaged.

Integrated analysis between LiDAR geometric and structural data and NDVI

As mentioned above, LiDAR data were summarized in points along the tree rows every 0.5 m (ROIs B). Then, to be compared with NDVI from Sentinel-2 and PlanetScope images, a geostatistical interpolation of each geometric and structural parameter derived from the LiDAR data was carried out using as grid points the center coordinates of each pixel from the images covering the study area. In this respect, only pixels that fully included center points of the ROIs B were considered (Figure 2). The interpolation was made using the software Variogram Estimation and Spatial Prediction with Error (VESPER, University of Sydney, Australia) (Minasny et al, 2005). Ordinary kriging was applied using linear with sill variograms. A total number of 4029 ROI B points were considered as input data. Then, LiDAR-derived parameters were interpolated on 690 central points of a 3 x 3 m grid for the PlanetScope image and on 53 central points of a 10 x 10 m grid in the case of the Sentinel-2 image.

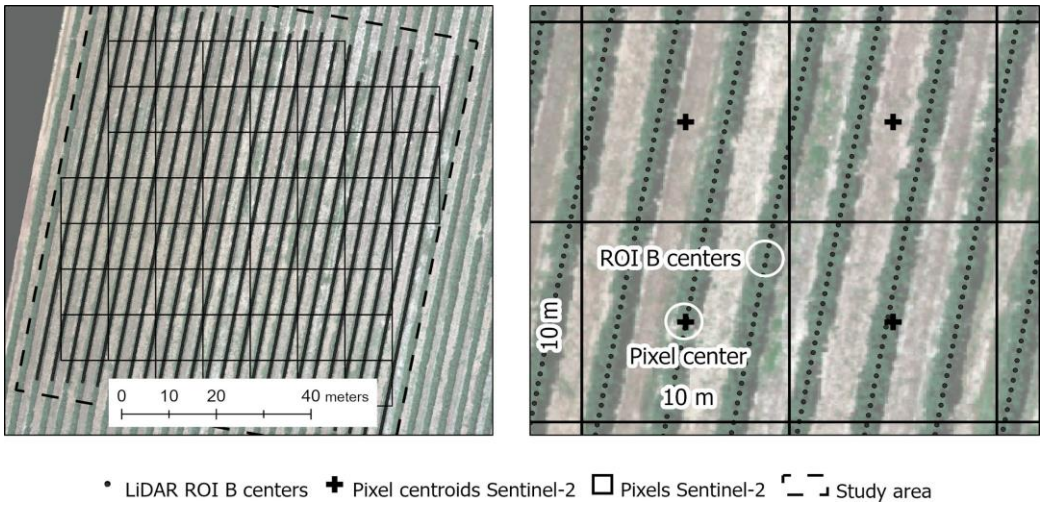

Figure 2. Graphical representation of the analysis setting to compare the LiDAR-derived geometrical and structural canopy parameters with the NDVI from the satellite images. Example for the Sentinel-2 image. Left: study area, rows of ROI B centers and pixels of Sentinel-2. Right: detail of ROI B centers and Sentinel-2 pixels with their centroids, where geometrical and structural LiDAR-derived parameters are interpolated. Background image is an aerial UAV image only used for better representation.

After the interpolation, all the LiDAR-derived geometric and structural properties and the NDVIs were referred to the respective grid centers (Sentinel-2 or PlanetScope pixel centroids), and were transferred to tables for further statistical analysis. In addition, all the maps of the properties were classified in 2 or 3 classes by means of the Isodata unsupervised classification algorithm in ArcGIS Pro (ESRI, Redlands, USA).

Statistical analysis

Two types of statistical analysis were carried out. On the one hand, a multivariate descriptive analysis was performed between the NDVI and the LiDAR-derived geometrical and structural data, obtaining the matrix of Pearson's linear correlation coefficients and their significance degree. For that, the software JMP Pro 14 (SAS Institute Inc., Cary, USA) was used. Next, the classified NDVI and LiDAR-derived parameters were spatially analized by means of the software Map Comparison Kit (MCK) (Visser & de Nijs, 2006). This program provides a good understanding of the differences between pairs of maps by means of the calculation of the Kappa index of agreement (Figure 3).

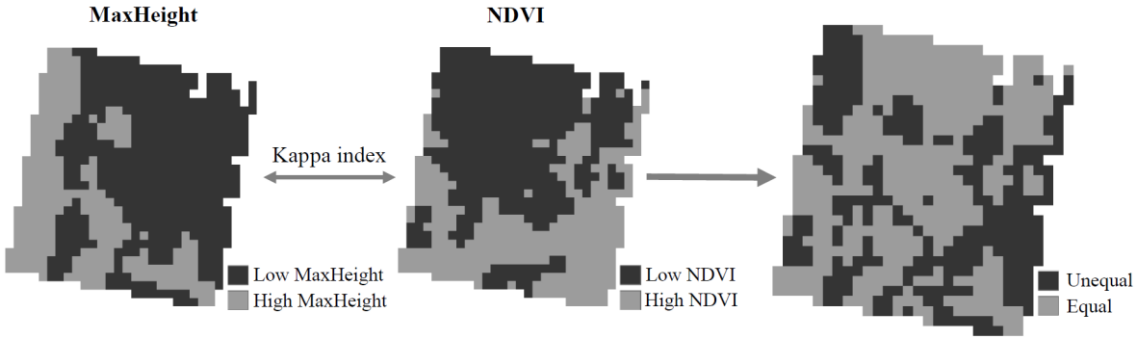

Figure 3. Example of the analysis of class maps and output with the software Map Comparison Kit. The figure shows the comparison between the MaxHeight and the NDVI referred to the pixels of the PlanetScope image.

Results

Multivariate descriptive analysis

Table 2 shows the results of the multivariate descriptive analysis between the NDVI and the LiDAR-derived geometric and structural canopy parameters for PlanetScope and Sentinel-2 images, respectively. The highest positive correlations were obtained between the NDVI of PlanetScope images and the SMaxWidth, MaxMaxWidth and the SChull, respectively. The Sentinel-2 NDVI showed the same pattern although with lower correlation values. As expected, porosity was negatively correlated in both cases, with higher values in the PlanetScope case.

Table 2. Multivariate descriptive analysis between NDVI from PlanetScope and Sentinel-2 and the LiDAR-derived geometric and structural canopy parameters. See description of variables in Table 1. Significance expressed as (**) p< 0.01, (*) p<0.05.

	MaxHeight	MaxWidth	MaxMaxWidth	Porosity-R	Porosity-L	Porosity-A	SMaxWidth	SChull
NDVI Planet	0.29**	0.64**	0.72**	-0.52**	-0.53**	-0.53**	0.74**	0.71**
NDVI Sentinel	0.37**	0.57**	0.50**	-0.42**	-0.31*	-0.37**	0.56**	0.57**

Comparison of classified maps

Table 3 summarizes the results of the Kappa index of agreement for the comparison between classified maps of the NDVI and the LiDAR-derived geometrical and structural parameters, either in 2 or 3 classes, after the classification with the Isodata algorithm.

Table 3. Kappa index of agreement between NDVI from PlanetScope and Sentinel-2 images and the LiDAR-derived geometric and structural canopy parameters. See description of variables in Table 1. 2C and 3C stand for 2 or 3 classes in the maps.

	MaxHeight	MaxWidth	MaxMaxWidth	Porosity-R	Porosity-L	Porosity-A	SMaxWidth	SChull
NDVI Planet 2C	0.16	0.35	0.46	-0.32	-0.39	-0.36	0.52	0.49
NDVI Planet 3C	0.11	0.34	0.41	-0.14	-0.11	-0.12	0.36	0.37
NDVI Sentinel 2C	0.12	0.34	0.39	-0.17	-0.18	-0.01	0.36	0.20
NDVI Sentinel 3C	-0.14	0.24	-0.01	-0.04	-0.09	-0.05	0.03	0.01

According to the criteria of Landis & Koch (1977), most of the analyzed map pairs showed either no agreement (Kappa < 0) or slight to fair agreement (0 < Kappa < 0.4). Only the SMaxWidth, Schull and MaxMaxWidth in the case of the PlanetScope derived NDVI and for the 2 classes maps, and the MaxMaxWidth for the 3 classes maps achieved a Kappa index in the range from 0.4 to 0.6 (Table 3), which represent fair to good agreement beyond chance.

Discussion

The present work was initially a challenge, since it is difficult to expect a correlation between parameters measured with very high accuracy, such as those derived from LiDAR data and a very simple, generic vegetation index such as NDVI obtained from satellite images with spatial resolutions of 3 or 10 m. However, the results are encouraging since correlation coefficients above 0.70 were obtained for relevant properties as the cross-sectional area along the tree rows of the super-intensive almond orchard (SMaxWidth and SChull) and the maximum width of the section (MaxMaxWidth). The results were better between LiDAR-derived data and PlanetScope

NDVI, whose images (PlanetScope) have about 11 times higher resolution than the Sentinel-2 one.

These findings are relevant because the cross-sectional area is an important parameter to determine the canopy volume and, hence, to optimize dose rates of plant protection products to apply in the orchard (Escolà et al., 2013); and it is also related to leaf density (Arnó et al., 2013). Nevertheless, the results of the spatial comparison of NDVI classes with the LiDAR-derived parameters only reached a moderate agreement beyond chance. Site-specific management of the orchard (i.e., application of plant protection products), on the basis of NDVI from satellite images should use the pixel size as reference unit rather than the NDVI classes.

As described in the introduction section, other authors have demonstrated the utility of remote sensing images, in particular from UAVs, to derive accurate geometric canopy parameters in orchards (Torres-Sánchez et al., 2018), or with the combination of geometric parameters and vegetation indices (Jurado et al., 2020). These are mainly based on measurements based on photogrammetric techniques and, in some cases, having LiDAR data as reference (Hobart et al., 2020). However, monitoring based on UAVs in relation to satellites, has the limitation of the frequency of image acquisition, and because of that the results of the present work can add value to the current knowledge.

Conclusions

The method evaluated in this work can complement the possibilities of canopy characterization in super-intensive orchards based on high temporal and spatial resolution satellite images. In this respect, vegetation parameters related to width and cross-sectional area of the canopy along the rows offered a high correlation with NDVI obtained from the evaluated images, in particular when PlanetScope images are used. Nevertheless, structural parameters as the porosity had no high correlations. This study has been based on data from a super-intensive almond orchard, but this methodology can be applied to other similar crops.

Acknowledgements

This work was funded by the Spanish Ministry of Science, Innovation and Universities through the project PAgFRUIT (RTI2018-094222-B-I00). The authors thank the Copernicus program for the use of Sentinel-2 images and Planet Labs Inc. for the use of PlanetScope images under the Educational and Research License agreement with the Universitat de Lleida.

References

Arnó, J., Escolà, A., Vallès, J.M., Llorens, J., Sanz, R., Masip, J., Palacín, J., Rosell-Polo, J.R. 2013. Leaf area index estimation in vineyards using a ground-based LiDAR scanner. Precision Agriculture 14, 290–306.

Bechar, A., & Vigneault, C. 2016. Agricultural robots for field operations: Concepts and components. Biosystems Engineering, 149, 94–111.

Colaço, A. F., Molin, J. P., Rosell-Polo, J. R., Escolà, A. 2018. Application of light detection and ranging and ultrasonic sensors to high-throughput phenotyping and precision horticulture: Current status and challenges. Horticulture Research, 5(1).

Escolà A, Rosell-Polo JR, Planas S, Gil E, Pomar J, Camp F, et al. 2013.Variable rate sprayer. Part 1 - Orchard prototype: Design, implementation and validation. Comput Electron Agric, 95,122–35.

Escolà, A., Martínez-Casasnovas, J. A., Rufat, J., Arnó, J., Arbonés, A., Sebé, F., Pascual, M., Gregorio, E., Rosell-Polo, J.R. 2017. Mobile terrestrial laser scanner applications in precision fruticulture/horticulture and tools to extract information from canopy point clouds. Precision Agriculture, 18(1), 111–132.

Hobart, M., Pflanz, M., Weltzien, C., & Schirrmann, M. 2020. Growth height determination of tree walls for precise monitoring in apple fruit production using UAV photogrammetry. *Remote Sensing*, *12*(10). https://doi.org/10.3390/rs12101656

Johansen, K., Raharjo, T., McCabe, M. 2018. Using Multi-Spectral UAV Imagery to Extract Tree Crop Structural Properties and Assess Pruning Effects. Remote Sensing, 10(6), 854.

Jurado, J. M., Ortega, L., Cubillas, J. J., Feito, F. R. 2020. Multispectral mapping on 3D models and multi-temporal monitoring for individual characterization of olive trees. Remote Sensing, 12(7).

Landis, J.R., Koch, G.G. 1977. The Measurement of Observer Agreement for Categorical Data. Biometrics, 33, 159-174.

Llorens, J., Cabrera, C., Escolà, A., Arnó, J. 2019. R software code to process and extract information from 3D Lidar point clouds. In: Poster Proceedings of the 12th European Conference on Precision Agriculture, July 8-11, Montpellier, France. pp. 114. e-book publication. SupAgro Montpellier. ISBN 978-2-900792-49-0.

Lorite, I. J., Cabezas-Luque, J. M., Arquero, O., Gabaldón-Leal, C., Santos, C., Rodríguez, A., Ruiz-Ramos, M., Lovera, M. 2020. The role of phenology in the climate change impacts and adaptation strategies for tree crops: a case study on almond orchards in Southern Europe. Agricultural and Forest Meteorology, 294, 108142.

Minasny, B., McBratney, A.B., and Whelan, B.M., 2005. VESPER version 1.62. Australian Centre for Precision Agriculture, The University of Sydney, NSW 2006. (http://www.usyd.edu.au/su/agric/acpa)

Planet. 2016 Planet imagery product specification: planetscope & rapideye. https://www.planet.com/products/satellite-imagery/files/1610.06_Spec%20Sheet_Combined_Imagery_Product_Letter_ENG v1.pdf. (last accessed 06/12/20)

Rouse, J.W. Jr, Haas, R.H., Deering, D.W., Schell, J.A., Harlan, J.C. 1974. Monitoring the Vernal Advancement and Retrogradation (GreenWave Effect) of Natural Vegetation, NASA/GSFC Type III Final Report: Greenbelt, MD, USA, 371p.

Sentinel user handbook 2015. https://sentinel.esa.int/documents/247904/685211/Sentinel-2_User_Handbook. (last accessed 06/12/20)

Torres-Sánchez, J., de Castro, A. I., Peña, J. M., Jiménez-Brenes, F. M., Arquero, O., Lovera, M., López-Granados, F. 2018. Mapping the 3D structure of almond trees using UAV acquired photogrammetric point clouds and object-based image analysis. Biosystems Engineering, 176, 172–184.

Vázquez-arellano, M., Griepentrog, H. W., Reiser, D., Paraforos, D. S. 2016. 3-D imaging systems for agricultural applications: A review. Sensors, 16 (5), 618.

Visser, H., de Nijs, T. 2006. The Map Comparison Kit. Environmental Modeling & Software 21, 346-358.